



HAL
open science

Nonlinear vibrations of an inclined cable

Alain Berlioz, Claude-Henri Lamarque

► **To cite this version:**

Alain Berlioz, Claude-Henri Lamarque. Nonlinear vibrations of an inclined cable. *Journal of Vibration and Acoustics*, 2005, 127 (4), pp.315-323. 10.1115/1.1924638 . hal-00814591

HAL Id: hal-00814591

<https://hal.science/hal-00814591v1>

Submitted on 18 Oct 2024

HAL is a multi-disciplinary open access archive for the deposit and dissemination of scientific research documents, whether they are published or not. The documents may come from teaching and research institutions in France or abroad, or from public or private research centers.

L'archive ouverte pluridisciplinaire **HAL**, est destinée au dépôt et à la diffusion de documents scientifiques de niveau recherche, publiés ou non, émanant des établissements d'enseignement et de recherche français ou étrangers, des laboratoires publics ou privés.



Distributed under a Creative Commons Attribution - NonCommercial 4.0 International License

Nonlinear Vibrations of an Inclined Cable

A. Berlioz¹

Laboratoire de Dynamique des Machines et des Structures CNRS UMR-5006, Institut National des Sciences Appliquées de Lyon, Villeurbanne, France

C-H. Lamarque

Laboratoire de GéoMatériaux CNRS URA-1652, Ecole Nationale des Travaux Publics de l'Etat, Vaulx-en-Velin, France

The goal of this experimental and theoretical study is to highlight the nonlinear dynamic behavior of an inclined cable consisting of a steel wire surrounded by copper wire. Measurements around the first frequency of vibration of the cable in and out of plane and around the second harmonic of this frequency were also carried out. These experimental results are in good agreement with the numerical results obtained via the multiple scale method applied to finite (1- and 2- degree-of-freedom (DOF) models). In order to prepare further investigations related to more complicated behavior, a 4-DOF model is added.

Introduction

Stayed girder bridges are very widely used structures. Currently, their dimensioning is generally carried out by using computer finite element codes and is primarily studied via static or linear dynamic approaches. However, certain resonance phenomena that permit the prediction of strongly nonlinear behavior have been observed in the cables of this type of structure. Given the current trend of constructing stayed bridges with longer spans and with increasingly greater attention placed on them, taking into account nonlinear phenomena appears essential. The carrying cables with stays are tilted, contrary to those of suspension bridges and they are embedded in the pillars of the bridge at their higher end. Furthermore, they are subjected to excitation because of the deck of the bridge at their lower end.

Numerous works have been devoted to the study of cable vibrations. First, Irvine and Caughey [1] considered a simplified linear model, but they did not take into account the quadratic and cubic terms of the partial differential equations governing the three-dimensional vibrations of a cable. In [2], Irvine studied a linear model that permitted him to solve the vibration problem completely and introduced the nonlinear model of a taut flat cable, though without solving it. Meirovitch [3] showed that the undamped nonlinear steady state in a plane response of a taut flat cable is given by the solution of a Duffing equation. West et al. [4] and Henghold and Russel [5] also studied natural frequencies of cable structures. Hence it is clear that cable vibrations have to be studied in the framework of nonlinear mechanics.

Nayfeh and Mook [6] recalled the basic modeling for strings and provide many references on the topic, whereas Takahashi and Konishi [7,8] presented nonlinear free vibrations and forced responses for a three-dimensional case. Benedettini et al. [9], El-Attar et al. [10], and Luongo et al. [11] studied planar nonlinear oscillations of an elastic cable suspended between two fixed supports at the same level under several different resonance conditions and presented experimental, analytical, and numerical results. In [12], Rega et al. considered multimodal resonances in a suspended cable studied via a perturbation approach, whereas Lilien and Pinto da Costa [13] investigated vibrations due to the parametric excitation of a cable-stayed structure. Fujino et al. [14] built a 3-DOF model of a cable-stayed beam and compared the results of analytical approaches to experimental results working on his Ph.D. thesis, and Khadraoui [15] proposed several models of simplified cable-stayed bridges with at most 3-DOF. In particu-

lar, he introduced a 1-DOF model of an inclined cable subjected to an external excitation corresponding to the movement of the deck of the bridge. In this paper we use a revised version of the simplified model given by [15], where the first harmonic external excitation was simplified [16].

In [17], Zhao et al. dealt with a 2-DOF model of an inclined cable for a theoretical investigation of in-plane and out-of-plane motions approximated by the first in-plane and out-of-plane modes.

By contrast with the above works, here we consider an inclined cable subjected to external sinusoidal forcing, leading to primary and subharmonic resonances.

The work presented concerns models with a few degrees of freedom obtained by projection of the continuous model onto a finite number of linear modes and the (quantitative) comparison between experimental investigations of planar motions and analytical results obtained for the simplified 1-DOF nonlinear model.

The setup corresponds to a cable in isolation excited by the deck of the bridge. In this study, the harmonic stress exerted on the cable of the setup corresponds to the effect of linear coupling and linear response of the deck.

Additional experimental results for planar and nonplanar motions are also reported. Analytical models for the analyses of two (with internal resonance [18]) and four degrees of freedom are given to prepare an analysis of the experimental results. This work follows on from and improves previous work [19]:

- Experimental results related to in-plane primary resonance and in-plane subharmonic resonance have been refined.
- Out-of-plane motions and couplings have been investigated experimentally.
- Experimental and numerical results have been compared for primary resonance out-of-plane behavior.
- Theoretical results are presented in [18], whereas this paper contains experimental investigations.

Theoretical Models

Several models are proposed and tested in the present paper. They are classified as: (i) a simplified model with one degree of freedom, (ii) a model with two degrees of freedom (one in the vertical plane and one in the transverse plane); and (iii) a model with four degrees of freedom (two in the vertical plane and two in the transversal plane). All of them involve only symmetric modes in accordance with the experimental observations reported in this paper.

The multiple scale method in time is used, and the theory is briefly recalled here.

Simplified Model With One Degree of Freedom. Using Irvine's function [1] for the first spatially symmetric planar mode

¹Now at Laboratoire de Génie Mécanique de Toulouse EA814, Université Paul Sabatier, 31062 Toulouse Cedex 4, France

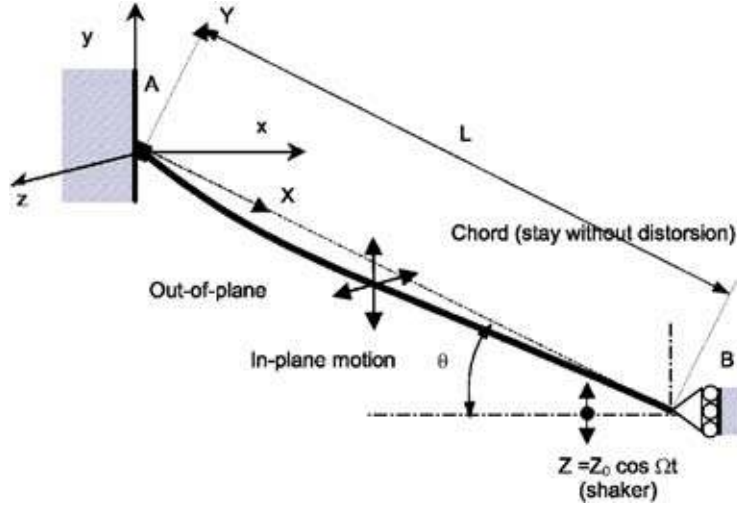


Fig. 1 Cable diagram

$$f(X) = \frac{\left[1 - \cos\left(\omega_0 \frac{X}{L}\right) - \tan\left(\frac{\omega_0}{2}\right) \sin\left(\omega_0 \frac{X}{L}\right) \right]}{\left[1 - \cos\left(\frac{\omega_0}{2}\right) - \tan\left(\frac{\omega_0}{2}\right) \sin\left(\frac{\omega_0}{2}\right) \right]} \quad (1)$$

and using adequate geometrical boundary conditions at the lower end B of the cable (see Fig. 1),

$$V(X, t) = f_y(X)\varphi(t) + \frac{X}{L}Z(t)\cos\theta \quad (2)$$

We consider the in-plane model with one degree of freedom established by Khadraoui (see [15]) obtained through the Ritz-Galerkin method and improved in [16]

$$\begin{aligned} \ddot{\varphi} + 2e\omega_0\dot{\varphi} + \omega_0^2\varphi + \tilde{b}_1\varphi^2 + \tilde{b}_2\varphi^3 + \tilde{b}_3\cos(\Omega t)\varphi + \tilde{b}_4\cos^2(\Omega t)\varphi \\ = \tilde{b}_5\cos(\Omega t) + \tilde{b}_6\cos^2(\Omega t) + \tilde{b}_7\sin(\Omega t) \end{aligned} \quad (3)$$

where $\varphi(t)$ is the unknown modal coordinate and

$$2e\omega_0 = \frac{Lc}{\sqrt{T_0m_c}} \quad \text{and} \quad \omega_0^2 = \frac{\tilde{C}_1}{\tilde{C}_0} + \xi \frac{\tilde{C}_2}{\tilde{C}_0} \quad (4)$$

The nondimensional constants $\tilde{b}_1 - \tilde{b}_7$ and $\tilde{C}_0 - \tilde{C}_2$ are given in Appendix A.

Damping c is introduced via a damping ratio. For such a cable the eigenfrequency is obtained from [15] with the transcendental relationship

$$tg\left(\frac{\omega_0}{2}\right) = \frac{\omega_0}{2} - \frac{4}{\lambda^2} \left(\frac{\omega_0}{2}\right)^3 \quad (5)$$

In what follows, the method of multiple scale time is used to investigate the 1-DOF model. Taking into account the effort of calculation, a development to the first order is used. In order to maintain the same contribution for the nonlinear terms and the damping effect, a small dimensionless parameter ε is used for both damping and nonlinear terms. Thus we introduce

$$e = \varepsilon e_0 \quad \text{and} \quad \tilde{b}_i = \varepsilon \tilde{b}_{i0} \quad \text{for } i = 1, \dots, 7 \quad (6)$$

Particular attention is paid to the primary and subharmonic resonances.

Primary Resonance for the 1-DOF Model. Let us assume the frequency expansion in the usual form

$$\Omega = \omega_0 + \varepsilon\sigma \quad (7)$$

The approximate solution obtained using the multiple scales in the time approach is

$$\varphi(t) = \rho \cos(\Omega t + \nu) + o(\varepsilon) \quad (8)$$

with the equilibrium equations

$$\begin{aligned} \omega_0(\Omega - \omega_0)\rho - 3\frac{\tilde{b}_2\rho^3}{8} - \frac{\tilde{b}_4}{8}\rho \cos(2\nu) - \frac{\tilde{b}_4}{4}\rho + \frac{\tilde{b}_5}{2}\cos(\nu) - \frac{\tilde{b}_7}{2}\sin(\nu) \\ = 0 \end{aligned} \quad (9)$$

$$-\omega_0^2 e \rho + \frac{\tilde{b}_4}{8}\rho \sin(2\nu) - \frac{\tilde{b}_5}{2}\sin(\nu) - \frac{\tilde{b}_7}{2}\cos(\nu) = 0 \quad (10)$$

Subharmonic Resonance for the 1-DOF System. In this case, parametric resonance occurs as was shown in [20]. However, since an inclined cable is considered, the coefficients of Eqs. (3), (9), and (10) are different from the horizontal or vertical cables. Moreover, new terms, such as those related to coefficients b_3 , occur. Assuming the frequency expansion of the form

$$\Omega = 2\omega_0 + \varepsilon\sigma \quad (11)$$

the multiple scales in time approach leads to

$$\varphi(t) = \rho \cos\left(\frac{\Omega}{2}t + \nu\right) + o(\varepsilon) \quad (12)$$

where the equilibrium equations are

$$\frac{(\Omega - 2\omega_0)\omega_0\rho}{2} - 3\frac{\tilde{b}_2\rho^3}{8} - \frac{\tilde{b}_4}{4}\rho - \frac{\tilde{b}_3}{4}\cos(2\nu)\rho = 0 \quad (13)$$

$$-\omega_0^2 e \rho + \frac{\tilde{b}_3}{4}\rho \sin(2\nu) = 0 \quad (14)$$

We must note that a trivial solution for the equilibrium position is given by $\rho=0$. Equations (13) and (14) give

$$tg(2\nu) = \frac{\omega_0^2 e}{\frac{(\Omega - 2\omega_0)\omega_0}{2} - 3\frac{\tilde{b}_2\rho^2}{8} - \frac{\tilde{b}_4}{4}} \quad (15)$$

Nontrivial solutions are obtained from

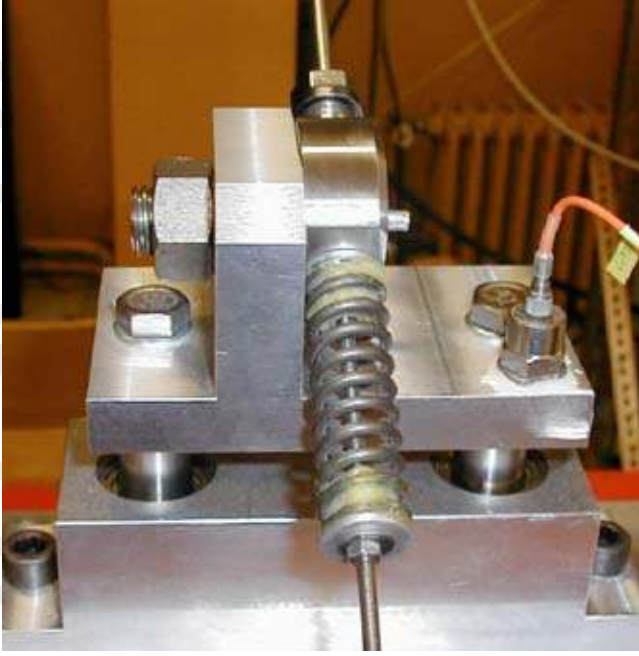


Fig. 2 Primary resonance, amplitude at $X=L/2$ versus external frequency: fitted (o-o), experimental (♦)

$$\frac{\rho^2}{2} = \frac{2(\Omega - 2\omega_0)\omega_0 - \tilde{b}_4 \mp \sqrt{\tilde{b}_3^2 - 16(\omega_0^2 e)^2}}{3\tilde{b}_2} \quad (16)$$

with the condition

$$\frac{\tilde{b}_3}{16} - (\omega_0^2 e)^2 \geq 0 \quad (17)$$

where b_3 is the parametric term in Eq. (3). Therefore, for given values of the system parameters, the system may have one or two real solutions for amplitude ρ (see Fig. 2) and the stability of solutions can be studied in classical manner.

Model With 2-DOF (In-Plane and Out-of-Plane). Using the same procedure, a model of a cable with two degrees of freedom is derived. It includes the first in-plane (see Eqs. (1) and (2)) and the first out-of-plane modes, which take the following form [2]

$$W(X,t) = f_z(X)\varphi_z(t) \quad (18)$$

$$f_z(X) = \sin\left(\frac{\pi X}{L}\right) \quad (19)$$

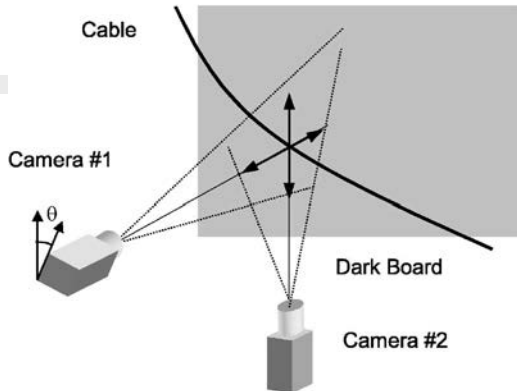


Fig. 3 Subsystem for initial tension force in the cable

Thus, the equations of motion are

$$\begin{aligned} \ddot{\varphi}_y + a_1\dot{\varphi}_y + a_2\varphi_y + a_3\cos(\Omega t)\varphi_y + a_4\cos^2(\Omega t)\varphi_y + a_5\varphi_y^3 + a_6\varphi_y^2 \\ + a_7\varphi_z^2 + a_8\varphi_z^2\varphi_y = -a_9\cos(\Omega t) - a_{10}\cos^2(\Omega t) - a_{11}\Omega \sin(\Omega t) \\ - a_{12}\Omega^2\cos(\Omega t) \end{aligned} \quad (20a)$$

$$\begin{aligned} \ddot{\varphi}_z + b_1\dot{\varphi}_z + b_2\varphi_z + b_3\cos(\Omega t)\varphi_z + b_4\cos^2(\Omega t)\varphi_z + b_5\varphi_z^3 + b_6\varphi_y\varphi_z \\ + b_7\varphi_y^2\varphi_z = 0 \end{aligned} \quad (20b)$$

where $\varphi_y(t)$ and $\varphi_z(t)$ are the unknown modal coordinates. The nondimensional constants a_1 – a_{12} , b_1 – b_7 are given in Appendix B. Examining the secular terms, it can be seen that resonances could occur for

$$\begin{aligned} \Omega &\approx \sqrt{a_2} \\ \Omega &\approx 2\sqrt{a_2} \\ \Omega &\approx \sqrt{a_2}/2 \\ \Omega &\approx \sqrt{b_2} \\ \Omega &\approx 2\sqrt{b_2} \end{aligned} \quad (21)$$

In this paper we focus our interest on primary and subharmonic resonances only.

Primary Resonance for the 2-DOF Model. In order to maintain the same contribution for the nonlinear terms and the damping effect, a small dimensionless parameter ε is used for both damping and nonlinear terms. Thus we introduce the following scaling of the parameter versus ε :

$$a_i = o(\varepsilon) \quad (22a)$$

for $i=1,3,\dots,12$

$$b_i = o(\varepsilon) \quad (22b)$$

for $i=1,3,\dots,7$

It is assumed that frequencies ω_p and ω_{op} of the in-plane and out-of-plane, respectively, are close to each other, thus we introduce

$$\omega_p = \sqrt{a_2} \quad \text{and} \quad \omega_{op} = \sqrt{b_2} = \sqrt{a_2} + \varepsilon\nu \quad (23)$$

The primary resonance corresponds to

$$\Omega = \omega_p + \varepsilon\sigma \quad (24)$$

and using the multiple scales-in-time method leads to first harmonic expressions of solutions for in-plane and out-of-plane modes, respectively, in the form

$$\varphi_y \approx a \cos(\Omega t + \alpha) \quad \text{and} \quad \varphi_z \approx b \cos(\Omega t + \beta) \quad (25)$$

where a , b , α , and β must verify

$$\begin{aligned} a\omega_p(\Omega - \omega_p) - \frac{3}{8}a_5a^3 - \frac{1}{8}a_4a \cos(2\alpha) - \frac{1}{4}a_4a - \frac{1}{2}\cos(\alpha)(a_9 + \Omega^2a_{12}) \\ + \frac{1}{2}a_{11}\sin(\alpha)\Omega - \frac{1}{4}a_8ab^2 - \frac{1}{8}a_8ab^2\cos(2\alpha - 2\beta) = 0 \end{aligned} \quad (26a)$$

$$\begin{aligned} -\frac{1}{2}a_1a\omega_p + \frac{1}{8}a_4a \sin(2\alpha) + \frac{1}{2}\sin(\alpha)(a_9 + \Omega^2a_{12}) + \frac{1}{2}a_{11}\cos(\alpha)\Omega \\ + \frac{1}{8}a_8ab^2\sin(2\alpha - 2\beta) = 0 \end{aligned} \quad (26b)$$

$$\begin{aligned} b[\omega_p(\Omega - \omega_{op}) - \frac{3}{8}b_5b^2 - \frac{1}{8}b_4b \cos(2\beta) - \frac{1}{4}b_4 - \frac{1}{4}b_7a^2 - \frac{1}{8}b_7a^2\cos(2\alpha \\ - 2\beta)] = 0 \end{aligned} \quad (26c)$$

$$b[-\frac{1}{2}b_1\omega_p + \frac{1}{8}b_4\sin(2\beta) - \frac{1}{8}b_7a^2\sin(2\alpha - 2\beta)] = 0 \quad (26d)$$

In this case constant and second harmonic terms are not taken into account as it can be done because of quadratic nonlinearities (e.g., [6]). These equations show the existence of one (or several) solution(s) for which b is null (out-of-plane motion). Thus the

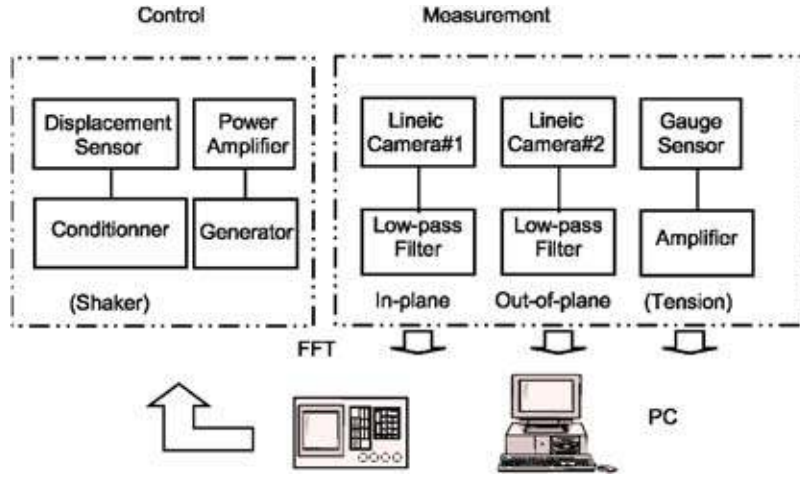


Fig. 4 Camera sensors and cable

canceling term b leads to an equation of the model with one degree of freedom capable of predicting the motion of the cable around its primary resonance. On the other hand, the combined motions (in-plane and out-of-plane) require the resolution of the four adapted equations.

Subharmonic Resonance for the 2-DOF System. Similarly, assuming that ω_p and ω_{op} are close

$$\Omega = 2\omega_p + \varepsilon\sigma \quad (27a)$$

we obtain the main harmonics of solutions in the form

$$\varphi_y \approx a \cos\left(\frac{\Omega}{2}t + \alpha\right) \quad \text{and} \quad \varphi_z \approx b \cos\left(\frac{\Omega}{2}t + \beta\right) \quad (27b)$$

with

$$a \left[\omega_p \left(\frac{\Omega}{2} - \omega_p \right) - \frac{3}{8}a_5a^2 - \frac{1}{4}a_4 - \frac{1}{4}a_3\cos(2\alpha) - \frac{1}{4}a_8b^2 - \frac{1}{8}a_8b^2\cos(2\alpha - 2\beta) \right] = 0 \quad (28a)$$

$$a \left[-\frac{1}{2}a_1\omega_p + \frac{1}{4}a_3\sin(2\alpha) + \frac{1}{8}a_8b^2\sin(2\alpha - 2\beta) \right] = 0 \quad (28b)$$

$$b \left[\omega_p \left(\frac{\Omega}{2} - \omega_{op} \right) - \frac{3}{8}b_5b^2 - \frac{1}{4}b_4 - \frac{1}{4}b_3\cos(2\beta) - \frac{1}{4}b_7a^2 - \frac{1}{8}b_7a^2\cos(2\alpha - 2\beta) \right] = 0 \quad (28c)$$

$$b \left[-\frac{1}{2}b_1\omega_p + \frac{1}{4}b_3\sin(2\beta) - \frac{1}{8}b_7a^2\sin(2\alpha - 2\beta) \right] = 0 \quad (28d)$$

The equations are similar (with respect to y and z), therefore, certain modes that are entirely localized on one plane or the other can occur. In these cases, the 1-DOF model is sufficient to predict the dynamic behavior of the cable. In addition, a null solution is also possible. However, for all the other solutions, the system composed of Eq. (28) needs to be solved.

Extension of the Finite-Degree-of-Freedom Model. More complicated models with several in-plane and out-of-plane modes could be introduced in a similar way. For example, a model including two in-plane and two out-of-plane modes can be considered. The modes are (see Eqs. (1), (2), (18), and (19)):

$$V(X,t) = f_{1y}(X)\varphi_{1y}(t) + f_{2y}(X)\varphi_{2y}(t) + \frac{X}{L}Z(t)\cos\theta \quad (29)$$

$$W(X,t) = f_{1z}(X)\varphi_{1z}(t) + f_{2z}(X)\varphi_{2z}(t) \quad (30)$$

and taking

$$f(X) = \sin\left(\frac{2\pi X}{L}\right) \quad (31)$$

as a common function for the second mode shape for in-plane and out-of-plane modes, too. Solving the entire system is rather painstaking, so the method is presented in Appendix C for only one equation. The method can be applied to other equations without difficulty.

Using the multiple scales time method leads to a system of eight equations after which the study of secular terms leads for example to the following possible resonances

$$\begin{array}{cccc} \omega_{1p} & \omega_{1op} & \omega_{2p} & \omega_{2op} \\ 2\omega_{1p} & 2\omega_{1op} & 2\omega_{2p} & 2\omega_{2op} \\ \omega_{1p} + \omega_{1op} & (\omega_{1p} + \omega_{1op})/2 & & \end{array} \quad (32)$$

and also other potential resonant combinations (see Eq. (C5)). It appears that some of them can be found in the range of interest.

Experimental Setup

In this section, the experimental setup used for testing the model and the demonstration of the main phenomenon (presented in [16]) are described. The main characteristics are shown in Table 1. The cable was composed of a steel wire surrounded by copper wire. This structure had a relatively heavy weight per unit length and low flexural rigidity.

At point A (see in Fig. 1), a strain-gage sensor was inserted between the end of the cable and the fixed anchorage and connected to a signal-conditioning amplifier, while a digital voltmeter was used to measure the static component of the axial force. The signal was plotted on a scope and recorded.

Table 1 Main characteristics of the setup

Length of cable	$L=1.905$ m
Weight per unit length	$m_c=0.177$ kg/m
Inclination angle	$\theta=27.5$ deg
Initial tension	$80 \text{ N} < T_0 < 200 \text{ N}$
Driven amplitude	$0.025 \text{ mm} < Z_0 < 0.150$
Frequency	$5 \text{ Hz} < \Omega < 25 \text{ Hz}$

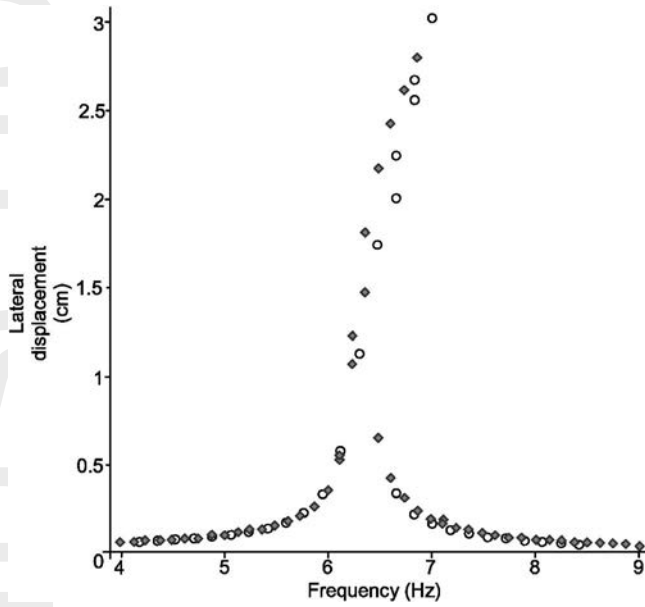


Fig. 5 Block diagram of the experimental setup

At the lower end, a 4700N Gearing & Watson shaker was used to apply the base excitation, matching the imposed displacement of the roadway of the bridge (deck).

The shaker was powered by a power control unit (G&W DS4) and a function generator (HP33120A). The displacement of the head of the shaker was monitored and held constant by an accelerometer.

The initial tension in the cable was applied with a specific subsystem composed of a thread, nut, and compression spring (see in Fig. 3). In the working configuration, the subsystem was mechanically locked on the moving part. We note that, because of gravity, the cable was slightly bent in the static configuration and the initial tension was 4N.

Displacements along vertical and horizontal directions in the middle of the cable were measured with two optolineic cameras located at this point. The cameras were equipped with a hardware-implemented peak detector to locate the displacements of the cable with respect to a reference point (see in Fig. 4). Measurements were acquired, displayed on a scope, and stored in real time at a sampling time of 1/500 s.

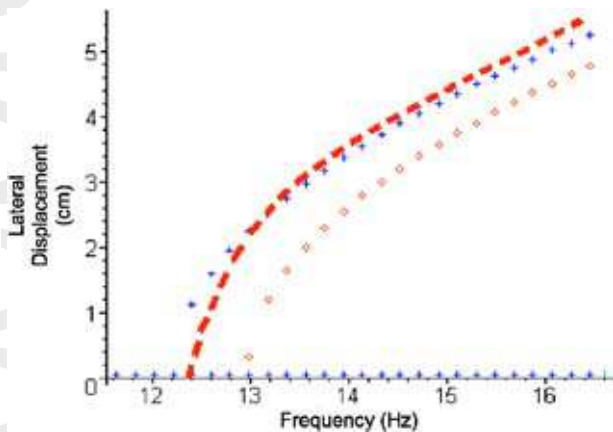


Fig. 6 Subharmonic resonance, amplitude at $X=L/2$ versus external frequency, $T_0=80$ N, $Z_0=3 \times 10^{-4}$ m: analytical stable branch (+), analytical unstable branch (□), and experimental (-)

Table 2 Experimental and numerical results

	Estimated	Experiment
T_0	80 N	80 N
Z_0	0.05 mm	0.05 mm
ω_0	6.3 Hz	6.1 Hz
e	0.6%	0.3–0.5 %

A low-pass filter (9002 Frequency Devices) was used to filter and magnify the signal from a 4096 pixel-cell camera. The accuracy of the signal measured depended to a large extent on the quality of the lenses, the distance between the camera and cable, the cable-board contrast, and the amplification of the low-pass filter. In testing mode, a spotlight was used to light the cable while a dark board was placed behind it (see in Fig. 5).

Results

The first linear natural frequencies of the cable were obtained using a classical impulse (low-amplitude) response by measuring the frequency spectra. A similar test was used to measure the damping ratio for several initial tensions.

Primary Resonance: Theory (1-DOF)-Experiment Comparison for In-Plane Motions. The behavior is weakly nonlinear and, from an experimental point of view, it is possible to observe alternately the first in-plane or out-of-plane mode vibration of the cable for low frequencies (from 5 to 10 Hz) under certain conditions. Since we focus on the in-plane mode only, certain specific initial conditions may be applied at the beginning of the procedure before obtaining a nonlinear stabilized in-plane vibration motion, then the control parameter (the excitation frequency) is slowly increased (or decreased).

The classical hysteretic phenomenon is clearly observed. The quantitative agreement can be obtained if the influence of damping and nondimensional parameter ξ_0 is considered attentively. In fact ξ_0 cannot be calculated very precisely from the theoretical expressions occurring in the model and the measurements taken from the experimental device. Thus, in order to compare experimental and theoretical results, a procedure is introduced to set a correct parameter ξ_0 and correct damping in the theoretical model. Therefore ξ_0 is calibrated for the theoretical curve from the experimental results.

The theoretical eigenfrequency ω_0^2 is estimated from the experimental curve with ξ_0 computed with Eq. (4) so that the maximal amplitudes are in good agreement. Then the damping is also estimated in the theoretical model to calibrate the maximal amplitude of the vibrations. Damping was also measured by logarithmic decrement from measurement data. The measured and identified parameters are presented in Table 2. The experimental parameters are those that were measured on the setup while the estimated parameters are deduced from measured data by using mathematical procedures.

For example, c and ω_0 were first obtained by measuring the cable's response to a small impulse test. Using the model determined by Eqs. (9), (10), and (4) for ξ with coefficients \tilde{b}_2 , \tilde{b}_4 , \tilde{b}_5 , and \tilde{b}_7 obtained from the measurements of γ and the computed values of \tilde{C}_0 , \tilde{C}_1 , \tilde{C}_2 , and \tilde{C}_3 , the optimal values of c and ω_0 are retrofitted in order to reduce the distance between the experimental curve (Fig. 2) and the solution of Eqs. (9) and (10). As can be seen in Table 2, there is slight difference between the "estimated" and "measured" values.

Good quantitative agreement was then obtained between the experiments and results of the model with identified parameters. See Fig. 2, where the measured and computed amplitudes at the middle of the cable ($L/2$) are plotted versus the frequency Ω of the external periodic stresses.

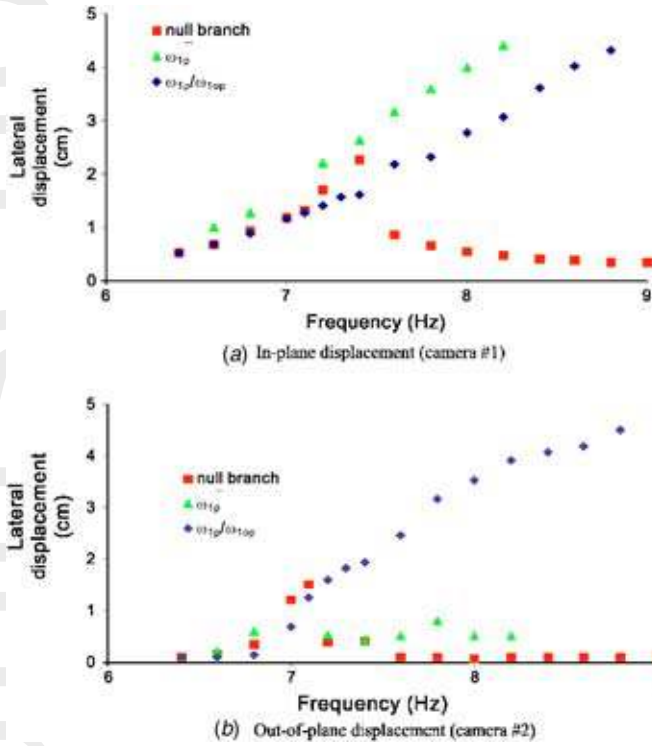


Fig. 7 Primary resonance, amplitude at $X=L/2$ versus external frequency, $T_o=120$ N, $Z_o=0.25$ mm: (a) In-plane displacement (camera 1) and (b) Out-of-plane displacement (camera 2)

Subharmonic Resonance: Comparison Between Theory (1 DOF) and Experiment for in-plane Motions. Several experiments were performed and good qualitative agreements were observed in all cases. Good quantitative agreement can be obtained by ensuring that tension, damping and Z_o do not vary during the experiment. In practice it is difficult to ensure this constancy. For example, for $T_o=130$ N, $Z_o=0.15$ mm, $e=3\%$ and ξ_o (calculated during experiments), small fluctuations occur so that Z_o is in the range [0.15–0.155 mm] and T_o in the range [130–135 N]. Thus the eigenfrequency measured is 7.4 Hz (theoretical value: 7.2 Hz).

The results for this type of experiment are given in Fig. 6, where the amplitude (at $L/2$) is plotted versus Ω . Good quantitative agreement is obtained. It should be noted that in some cases, the experimental branch becomes unstable because of the occurrence of other in-plane or out-of-plane vibrations.

Additional Experimental Results. Many other experimental results were obtained. A few of them are reported hereafter. In particular, vibration amplitudes measured at the cable's midpoint are presented under several amplitudes of external stresses Z_o .

Primary Resonance. Three types of stable motions were observed:

- Quasinull in-plane motion and null out-of-plane motion (null branch) (see in Figs. 7(a) and 7(b)). The null branch of Fig. 7(a) corresponds to the response of the system when increasing Ω , whereas the null branch of Fig. 7(b) corresponds to the response when decreasing Ω . Perturbations occurring during experiments cause the displacements to be not strictly equal to zero.
- Combined in-plane and out-of-plane motion (ω_{1p}/ω_{1op}) was observed only for “high” Z_o (see in Figs. 8(a) and 8(b)).
- Essentially in-plane motion that reaches amplitudes higher than the previous one ($\omega_{1p}/0$).

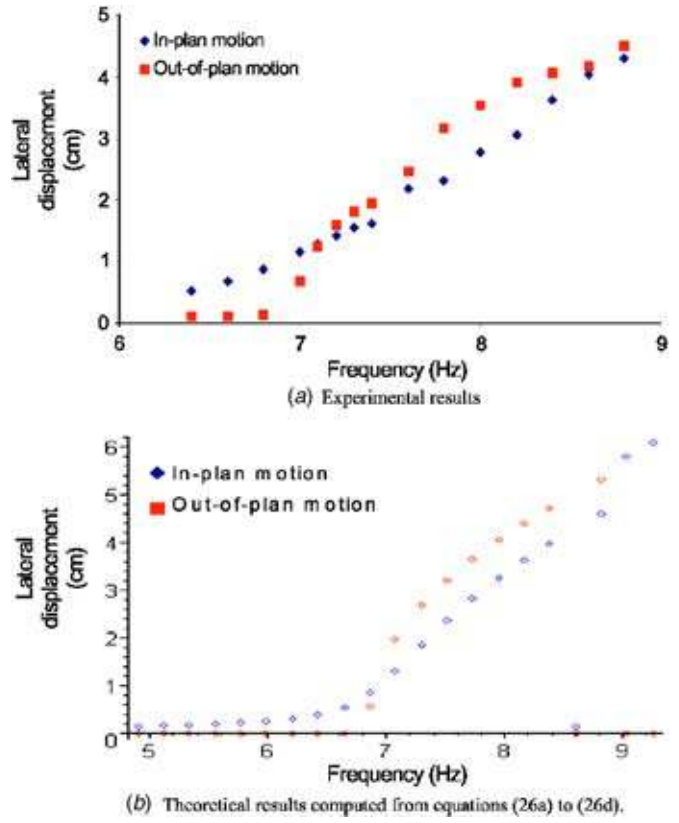


Fig. 8 Combination of in-plane and out-of-plane motions. Primary resonance, large Z_o . In-plane (\diamond), out-of-plane (\blacksquare): (a) experimental results and (b) theoretical results computed from Eqs. (26a)–(26d).

Contrary to the in-plane motion, the out-of-plane motion corresponds either to a resonance or to a completely null displacement. It seems that this phenomenon can be explained by the equations obtained for the 2-DOF model.

Using the theoretical 1-DOF model, we verified that the two in-plane motions (null branch and ω_{1p}/ω_{1op} branch) of the cable corresponded to the theoretical predictions carried out by this simple model.

For this type of combined vibration, in-plane displacements were similar to those observed for purely in-plane displacements if the maximal amplitude was rather weak (far from resonance behavior). The maximal amplitudes at resonance were lower than for the purely in plane vibration.

Furthermore, out-of-plane motions corresponding to the following phenomena were observed (see in Figs. 8(a) and 8(b)):

- When increasing external frequency, out-of-plane displacement is first null, then increases from one frequency value greater than (but close to) ω_{op} so that the out-of-plane amplitudes become as high as the in-plane ones.
- When decreasing the frequency from the highest previous values to smaller ones, the out-of-plane displacement is almost null in the neighborhood of ω_{op} .

Sub Harmonic Results. In this case, four types of vibrations can be observed whatever the amplitude of external stress (see Figs. 9(a) and 9(b)):

- null motion (in-plane and out-of-plane: trivial branch)
- subharmonic motion of the first in-plane mode ($2\omega_{1p}/0$)

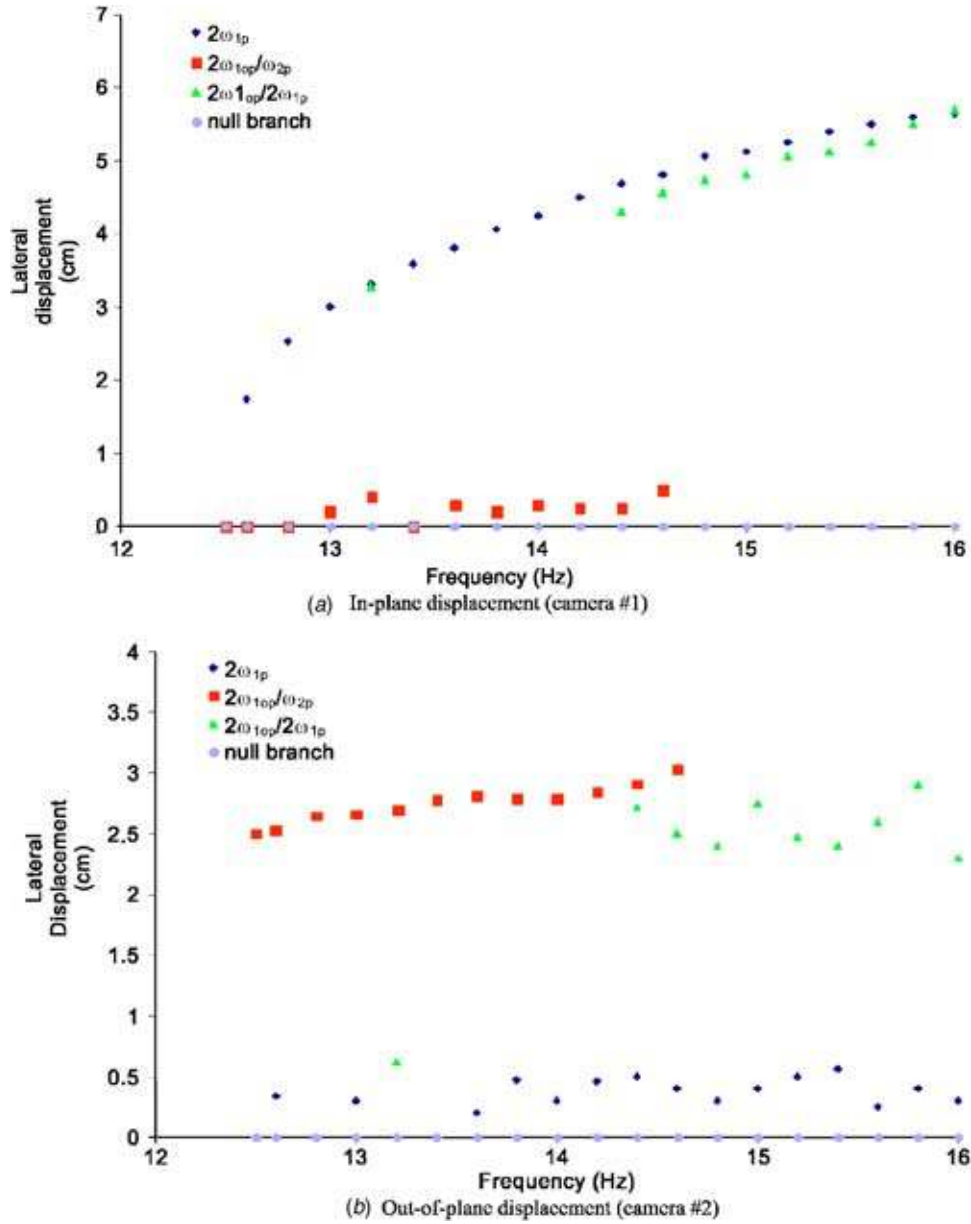


Fig. 9 Sub-harmonic resonance, amplitude at $X=L/2$ versus external frequency: (a) in-plane displacement (camera 1) and (b) out-of-plane displacement (camera 2)

- combination of subharmonic motion of the first in-plane mode and of the subharmonic motion of the first out-of-plane mode ($2\omega_{1p}/2\omega_{1op}$),
- combination of the subharmonic motion of the first out-of-plane mode with the second in-plane mode ($\omega_{2p}/2\omega_{1op}$).

All the types of resonances observed could be predicted using the 4-DOF model. Further numerical and experimental investigations are needed to describe other resonance cases.

Conclusion

This paper presented a modified model for the dynamic behavior of an inclined cable. Both primary and subharmonic resonances were studied from a theoretical point of view by using the multiple scales in time method. The 1-DOF model is devoted to in-plane motion. It was extended to 2- and 4-DOF for in-plane and

out-of-plane motions (one or two modes in each plane, respectively). The models were validated experimentally on a specific device using a shaker and contactless sensors.

The results presented exhibit good agreement between theory and experiment, and several nonlinear motions were observed and identified under periodic external stresses. Future developments will deal with multiharmonic and stochastic excitations.

Acknowledgments

This study has been supported by the Rhône-Alpes Council under the project titled Emergence 2003. The authors would like to thank Franck Bourrier and Christophe Quesne who provided part of the experimental and numerical computation.

Appendix A: Coefficient for the Simplified Model With One Degree of Freedom

The first eigenfrequency ω_0 of the cable obtained from [7]

$$\operatorname{tg}\left(\frac{\omega_0}{2}\right) = \frac{\omega_0}{2} - \frac{4}{\lambda^2} \left(\frac{\omega_0}{2}\right)^3 \quad \text{and} \quad \lambda^2 = \frac{\xi_0 \eta_0^2}{1 + \frac{\eta_0^2}{8}} \quad (\text{A1})$$

with

$$\eta_0 = \frac{8\zeta}{\cos^2 \theta} \quad \text{and} \quad \gamma = \frac{\zeta}{L} \quad (\text{A2})$$

where ζ corresponds to the deflection at the middle of the cable.

Coefficients $\tilde{b}_1, \dots, \tilde{b}_7$ and $\tilde{C}_0, \dots, \tilde{C}_3$ are given by

$$\begin{aligned} \tilde{b}_1 &= \frac{3\tilde{C}_1\tilde{C}_2}{2\tilde{C}_0} \gamma \xi \\ \tilde{b}_2 &= \frac{\tilde{C}_1^2}{2\tilde{C}_0} \gamma^2 \xi \\ \tilde{b}_3 &= \frac{\tilde{C}_1}{\tilde{C}_0} \xi \gamma Z_0 \sin \theta \\ \tilde{b}_4 &= \frac{\tilde{C}_1}{2\tilde{C}_0} \xi \gamma^2 Z_0^2 \cos^2 \theta \\ \tilde{b}_5 &= \frac{Z_0}{\tilde{C}_0} (\tilde{C}_3 \Omega^2 \cos \theta - \tilde{C}_2 \xi \sin \theta) \\ \tilde{b}_6 &= -\frac{\tilde{C}_2}{2\tilde{C}_0} \xi \gamma Z_0^2 \cos^2 \theta \\ \tilde{b}_7 &= \frac{\tilde{C}_3}{\tilde{C}_0} 2e\omega_0 \Omega Z_0 \cos \theta \end{aligned} \quad (\text{A3})$$

$$\begin{aligned} \tilde{C}_0 &= \int_0^1 f^2(X) dX \\ \tilde{C}_1 &= \int_0^1 f'^2(X) dX \\ \tilde{C}_2 &= \int_0^1 f'(X) Y' dX \\ \tilde{C}_3 &= \int_0^1 X f(X) dX \end{aligned} \quad (\text{A4})$$

Appendix B: Coefficient for the Model With Two Degrees of Freedom

$$\begin{aligned} a_1 &= e_1 = c_1 \gamma \sqrt{\frac{T_0}{m_c}} \\ a_2 &= \frac{C_1}{C_0} + \xi \frac{C_2}{C_0} \\ a_3 &= \frac{C_1}{C_0} \xi \gamma Z_0 \sin \theta \\ a_4 &= \frac{C_1}{2C_0} \xi \gamma^2 Z_0^2 \cos^2 \theta \end{aligned}$$

$$a_5 = \frac{C_1^2}{2C_0} \gamma^2 \xi$$

$$a_6 = \frac{3C_1 C_2}{2C_0} \gamma \xi$$

$$a_7 = \frac{C_2 C_4}{2C_0} \gamma \xi$$

$$a_8 = \frac{C_1 C_4}{2C_0} \gamma^2 \xi$$

$$a_9 = \frac{Z_0}{C_0} C_2 \xi \sin \theta$$

$$a_{10} = \frac{C_2}{2C_0} \xi \gamma Z_0^2 \cos^2 \theta$$

$$a_{11} = -\frac{C_3}{C_0} e_1 Z_0 \cos \theta$$

$$a_{12} = -\frac{Z_0}{C_0} C_3 \cos \theta \quad (\text{B1})$$

For instance, it can be seen that in the case of an uncoupled motion, Eq. (20a) leads to Eq. (3) with

$$\tilde{b}_5 = -a_9 - a_{12} \Omega$$

$$b_1 = e_2 = c_2 \gamma \sqrt{\frac{T_0}{m_c}}$$

$$b_2 = \frac{C_4}{C_5}$$

$$b_3 = \frac{C_4}{C_5} \xi \gamma Z_0 \sin \theta$$

$$b_4 = \frac{C_4}{2C_5} \xi \gamma^2 \cos^2 \theta$$

$$b_5 = \frac{C_4^2}{2C_5} \gamma^2 \xi$$

$$b_6 = \frac{C_2 C_4}{C_5} \gamma \xi$$

$$b_7 = \frac{C_1 C_4}{2C_5} \gamma^2 \xi \quad (\text{B2})$$

$$C_0 = \int_0^1 f_y^2(X) dX$$

$$C_1 = \int_0^1 f_y'^2(X) dX$$

$$C_2 = \int_0^1 f_y'(X) Y' dX$$

$$C_3 = \int_0^1 X f_y(X) dX$$

$$C_4 = \int_0^1 f_z'^2(X) dX$$

$$C_5 = \int_0^1 f_z^2(X) dX \quad (B3)$$

Appendix C: Model With Four Degrees of Freedom

By ordering the coefficients with a small dimensionless parameter ε as

$$a_i = \varepsilon a_{i0} \quad \text{for } i = 1, 3, \dots, 22$$

$$b_i = \varepsilon b_{i0} \quad \text{for } i = 1, 3, \dots, 22$$

$$c_i = \varepsilon c_{i0} \quad \text{for all } i, d_i = \varepsilon d_{i0} \quad \text{for all } i$$

$$a_2 = a_{20}, b_2 = b_{20}, c_2 = c_{20} \quad \text{and} \quad d_2 = d_{20} \quad (C1)$$

we obtain a system of four equations

$$\begin{aligned} & \ddot{\varphi}_{1y} + a_1 \dot{\varphi}_{1y} + a_2 \varphi_{1y} + a_3 \cos(\Omega t) \varphi_{1y} + a_4 \cos^2(\Omega t) \varphi_{1y} + a_5 \varphi_{2y} \\ & + a_6 \cos(\Omega t) \varphi_{2y} + a_7 \varphi_{1y}^2 + a_8 \cos(\Omega t) \varphi_{1y}^2 + a_9 \varphi_{1y}^3 + a_{10} \varphi_{2y}^2 \\ & + a_{11} \varphi_{1z}^2 + a_{12} \varphi_{2z}^2 + a_{13} \varphi_{2y} \varphi_{1y} + a_{14} \cos(\Omega t) \varphi_{2y} \varphi_{1y} \\ & + a_{15} \varphi_{2y} \varphi_{1y}^2 + a_{16} \varphi_{2y}^2 \varphi_{1y} + a_{17} \varphi_{1z}^2 \varphi_{1y} + a_{18} \varphi_{2z}^2 \varphi_{1y} \\ & = -a_{19} \cos(\Omega t) - a_{20} \Omega^2 \cos(\Omega t) - a_{21} \Omega \sin(\Omega t) - a_{22} \cos^2(\Omega t) \end{aligned} \quad (C2a)$$

$$\begin{aligned} & \ddot{\varphi}_{2y} + b_1 \dot{\varphi}_{2y} + b_2 \varphi_{2y} + b_3 \cos(\Omega t) \varphi_{2y} + b_4 \cos^2(\Omega t) \varphi_{2y} + b_5 \varphi_{1y} \\ & + b_6 \cos(\Omega t) \varphi_{1y} + b_7 \varphi_{2y}^2 + b_8 \cos(\Omega t) \varphi_{2y}^2 + b_9 \varphi_{2y}^3 + b_{10} \varphi_{1y}^2 \\ & + b_{11} \varphi_{1z}^2 + b_{12} \varphi_{2z}^2 + b_{13} \varphi_{2y} \varphi_{1y} + b_{14} \cos(\Omega t) \varphi_{2y} \varphi_{1y} \\ & + b_{15} \varphi_{1y} \varphi_{2y}^2 + b_{16} \varphi_{1y}^2 \varphi_{2y} + b_{17} \varphi_{1z}^2 \varphi_{2y} + b_{18} \varphi_{2z}^2 \varphi_{2y} \\ & = -b_{19} \cos(\Omega t) - b_{20} \Omega^2 \cos(\Omega t) - b_{21} \Omega \sin(\Omega t) - b_{22} \cos^2(\Omega t) \end{aligned} \quad (C2b)$$

$$\begin{aligned} & \ddot{\varphi}_{1z} + c_1 \dot{\varphi}_{1z} + c_2 \varphi_{1z} + c_3 \cos(\Omega t) \varphi_{1z} + c_4 \cos^2(\Omega t) \varphi_{1z} + c_9 \varphi_{1z}^3 \\ & + c_{13} \varphi_{1y} \varphi_{1z} + c_{14} \varphi_{2y} \varphi_{1z} + c_{15} \varphi_{1y}^2 \varphi_{1z} + c_{16} \varphi_{2y}^2 \varphi_{1z} \\ & + c_{17} \varphi_{1y} \varphi_{2y} \varphi_{1z} + c_{18} \cos(\Omega t) \varphi_{1y} \varphi_{1z} + c_{19} \cos(\Omega t) \varphi_{2y} \varphi_{1z} \\ & + c_{20} \varphi_{2z}^2 \varphi_{1z} = 0 \end{aligned} \quad (C2c)$$

$$\begin{aligned} & \ddot{\varphi}_{2z} + d_1 \dot{\varphi}_{2z} + d_2 \varphi_{2z} + d_3 \cos(\Omega t) \varphi_{2z} + d_4 \cos^2(\Omega t) \varphi_{2z} + d_9 \varphi_{2z}^3 \\ & + d_{13} \varphi_{1y} \varphi_{2z} + d_{14} \varphi_{2y} \varphi_{2z} + d_{15} \varphi_{1y}^2 \varphi_{2z} + d_{16} \varphi_{2y}^2 \varphi_{2z} \\ & + d_{17} \varphi_{1y} \varphi_{2y} \varphi_{2z} + d_{18} \cos(\Omega t) \varphi_{1y} \varphi_{2z} + d_{19} \cos(\Omega t) \varphi_{2y} \varphi_{2z} \\ & + d_{20} \varphi_{1z}^2 \varphi_{2z} = 0 \end{aligned} \quad (C2d)$$

Equations of zero order show that

$$\varphi_{1y0} = A_a(T_1) e^{i\sqrt{a_{20}}T_0} + \bar{A}_a(T_1) e^{-i\sqrt{a_{20}}T_0}$$

$$\varphi_{2y0} = A_b(T_1) e^{i\sqrt{b_{20}}T_0} + \bar{A}_b(T_1) e^{-i\sqrt{b_{20}}T_0}$$

$$\varphi_{1z0} = B_a(T_1) e^{i\sqrt{c_{20}}T_0} + \bar{B}_a(T_1) e^{-i\sqrt{c_{20}}T_0}$$

$$\varphi_{2z0} = B_b(T_1) e^{i\sqrt{d_{20}}T_0} + \bar{B}_b(T_1) e^{-i\sqrt{d_{20}}T_0} \quad (C3)$$

Substituting these solutions into the four first-order equations,

$$\frac{\partial^2 y_1}{\partial T_0^2} + a_{20} y_1 = \frac{1}{8} a_{140} A_b \bar{A}_a e^{i(-\Omega + \sqrt{a_{20} - \sqrt{b_{20}}})T_0} - \frac{1}{8} a_{80} \bar{A}_a^2 e^{i(\Omega - 2\sqrt{a_{20}})T_0} \quad (C4)$$

Putative secular terms imply resonances if

$$\Omega = \sqrt{b_{20}} - 2\sqrt{a_{20}} = \omega_{2p} - 2\omega_{1p} \quad (C5)$$

$$\Omega = 3\sqrt{a_{20}} = \omega_{1p} \quad (C6)$$

References

- [1] Irvine, H. M., and Caughey, T. K., 1974, "The Linear Theory of Free Vibrations of a Suspended Cable," *Proc. R. Soc. London, Ser. A* **341**, pp. 299–315.
- [2] Irvine, H. M., 1981, *Cable Structures*, MIT Press, Cambridge, MA.
- [3] Meirovitch, L., 1975, *Elements of Vibration Analysis*, McGraw-Hill, NY.
- [4] West, H. H., Geschwindner, L. F., and Suhoski, J. E., 1975, "Natural Vibrations of Suspension Cables," *J. Struct. Div. ASCE* **ST11**, pp. 2277–2291.
- [5] Henghold, W. M., and Russell, J. J., 1976, "Equilibrium and Natural Frequencies of Cable Structures (A Nonlinear Finite Element Approach)," *Comput. Struct.* **6**, pp. 267–271.
- [6] Nayfeh, A. H., and Mook, D. T., 1979, *Nonlinear Oscillations*, Wiley, NY.
- [7] Takahashi, K., and Konishi, Y., 1987, "Nonlinear Vibrations of Cables in Three Dimensions, Part I: Nonlinear Free Vibrations," *J. Sound Vib.* **118**(1), pp. 69–84.
- [8] Takahashi, K., and Konishi, Y., 1987, "Nonlinear Vibrations of Cables in Three Dimensions, Part II: Out of Plane Vibrations Under In-Plane Sinusoidally Time-Varying Load," *J. Sound Vib.* **118**(1), pp. 85–97.
- [9] Benedettini, F., Rega, G., and Alaggio, R., 1995, "Nonlinear Oscillations of a Four-Degree-of-Freedom Model of a Suspended Cable Under Multiple Internal Resonance Conditions," *J. Sound Vib.* **182**(5), pp. 775–798.
- [10] El-Attar, M., Ghobarah, A., and Aziz, T. S., 2000, "Nonlinear Cable Response to Multiple Support Periodic Excitation," *Eng. Struct.* **22**, pp. 1301–1312.
- [11] Luongo, A., Rega, G., and Vestroni, F., 1984, "Planar Nonlinear Free Vibrations of Elastic Cable," *Int. J. Non-Linear Mech.* **19**(1), pp. 39–52.
- [12] Rega, G., Lacarbonara, W., Nayfeh, A. H., and Char-Ming, Chin, 1997, "Multimodal Resonances in Suspended Cables Via a Direct Perturbation Approach," *Proc. of ASME DETC1997, VIB-4101*, Sacramento, Sept. 14–17, ASME, New York.
- [13] Lilien, J. L., and Pinto da Costa, A., 1994, "Vibration Amplitudes Caused by Parametric Excitation of Cable Stayed Structure," *J. Sound Vib.* **174**(1), pp. 69–90.
- [14] Fujino, Y., Warnitchai, P., and Pacheco, B. M., 1992, "An Experimental and Analytical Study of Autoparametric Resonance in a 3 DOF Model of Cable-Stayed-Beam," *Nonlinear Dyn.* **4**, pp. 111–138.
- [15] Khadraoui, I., 1999, "Contribution à la Modélisation et à L'Analyse Dynamique des Structures à Câbles," *Thèse de Doctorat, Université d'Evry*, 262p, (in French).
- [16] Berlioz, A., Lamarque, C. H., and Malasoma, J. M., 2001, "Nonlinear Behavior of an Inclined Cable: Experimental and Analytical Investigations," *Proc. of ASME DETC2001, VIB-21557*, Pittsburgh, Sept. 9–12, ASME, New York.
- [17] Zhao, Y. Y., Wang, L. H., Chen, D. L., and Jiang, L. Z., 2002, "Nonlinear Dynamics Analysis of the Two-Dimensional Simplified Model of an Elastic Cable," *J. Sound Vib.*, **255**(1), pp. 43–59.
- [18] Triantafyllou, M. S., and Grinfolgel, L., 1986, "Natural Frequencies and Modes of Inclined Cables," *J. Struct. Eng.* **112**, pp. 139–148.
- [19] Berlioz, A., and Lamarque, C. H., 2004, "A Nonlinear Model for the Dynamics of an Inclined Cable," *J. Sound Vib.*, **279**(3–5), pp. 619–639.
- [20] Perkins, N. C., 1992, "Modal Interactions in the Nonlinear Response of Elastic Cables Under Parametric/External Excitation," *Int. J. Non-Linear Mech.* **27**(2), pp. 233–250.